

Electronic supporting information for:

**Self-assembly and surface behaviour of pure and mixed zwitterionic amphiphiles
in a deep eutectic solvent**

A. Sanchez-Fernandez,^{ab} G.L. Moody,^a L.C. Murfin,^a T. Arnold,^{a,b,c} A.J. Jackson,^{b,d} S.M. King,^e S.E. Lewis^a
and K.J. Edler^a

^aDepartment of Chemistry, University of Bath, Claverton Down, Bath, BA2 7AY, UK.

^bEuropean Spallation Source, SE-221 00, Lund, Sweden.

^cDiamond Light Source, Harwell Campus, Didcot OX11 0DE, UK.

^dDepartment of Physical Chemistry, Lund University, SE-221 00, Lund, Sweden.

^eISIS Pulsed Neutron & Muon Source, Harwell Campus, Didcot OX11 0QX, UK.

Synthesis and characterisation of surfactants

All chemicals and solvents used were reagent grade purchased from the following commercial suppliers: Sigma Aldrich, VWR Chemicals and Fischer Scientific. All chemicals and solvents purchased, unless otherwise stated, were used without further purification.

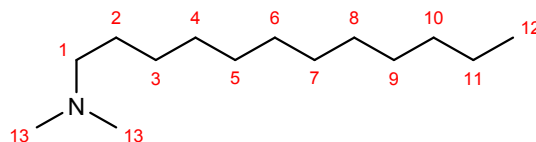
Unless stated otherwise, ambient conditions were used for each reaction. Inert conditions were achieved by using anhydrous solvents and by allowing the reaction to proceed under an atmosphere of nitrogen or argon.

All thin layer chromatography was performed using commercially available silica plates (pre-coated, aluminium backed). Visualisation was achieved through staining the plate with ammonium molybdate before gently heating.

All ^1H NMR and $^{13}\text{C}\{^1\text{H}\}$ NMR spectra were acquired on a Bruker 300 MHz spectrometer using chloroform-*d* as the reference ($\delta_{\text{H}} = 7.26$ ppm, $\delta_{\text{C}} = 77.0$ ppm). Chemical shifts (δ) are reported in parts per million. Coupling constants, *J* (Hz), are given where calculable.

High Resolution Mass Spectrometry (HRMS) was performed using a microTOF spectrometer with electrospray ionisation (ESI) used as the ionisation method.

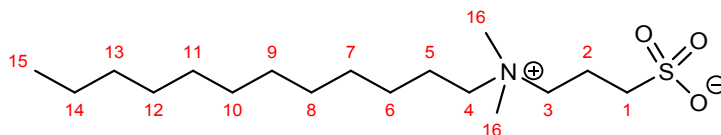
N,N-dimethyldodecan-1-amine



Under an atmosphere of nitrogen, 1-bromododecane (0.65 mL, 2.7 mmol, 1.0 eq) in ethanol (30 mL) was added dropwise to dimethylamine in an ethanolic solution (5.60 M, 4.80 mL, 27.0 mmol, 10.0 eq). The mixture was heated to 75°C for 21 hours. The excess solvent was evaporated under reduced pressure affording a creamy white solid which was diluted with NaOH (1 M, 60 mL) and extracted with hexane (3 × 60 mL). The combined organic extracts were dried over MgSO_4 , filtered, and the solvent removed under reduced pressure to give *N,N*-dimethyldodecan-1-amine as a pale yellow oil (0.47 g, 83%), used without purification.

^1H NMR (300 MHz, CDCl_3): $\delta_{\text{H}} = 2.31\text{--}2.18$ (8H, m, H^1 , H^{13}), 1.52–1.36 (2H, m, H^2), 1.37–1.16 (18H, m, $\text{H}^3 - \text{H}^{11}$), 0.85 (3H, t, *J* = 6.9 Hz, H^{12}); ^{13}C NMR (300 MHz, CDCl_3): $\delta_{\text{C}} = 60.1$, 45.6, 32.0, 29.80, 29.76, 29.7, 29.5, 27.9, 27.6, 22.8, 14.2; HRMS (ES): *m/z* = 214.2516; $\text{C}_{14}\text{H}_{32}\text{N}$ [$\text{M}+\text{H}$] $^+$ requires 214.2529. ^{13}C data¹ and ^1H NMR data² in agreement with those previously reported.

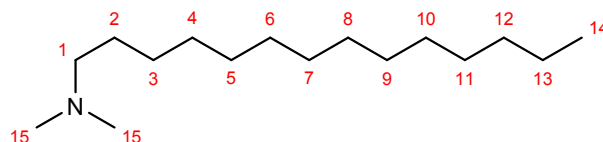
3-(dodecyldimethylammonio)propane-1-sulfonate



N,N-dimethyldodecan-1-amine (2.5 mL, 9.4 mmol, 1.0 eq) in acetone (15 mL) was added to a solution of 1,3-propanesultone (4.2 mL, 47 mmol, 5.0 eq) in acetone (20 mL) and refluxed for 5 hours. This afforded a white solid which was filtered at room temperature, washed with acetone and purified *via* recrystallisation with methanol and acetone to give 3-(dodecyldimethylammonio)propane-1-sulfonate as a white solid (2.50 g, 80%).

^1H NMR (300 MHz, CDCl_3): $\delta_{\text{H}} = 3.82\text{--}3.69$ (2H, m, H^3), 3.38–3.07 (8H, m, H^4 , H^{16}), 2.94 (2H, t, *J* = 6.7 Hz, H^1), 2.30–2.18 (2H, m, H^2), 1.79–1.63 (2H, m, H^5), 1.45–1.09 (18H, m, $\text{H}^6 - \text{H}^{14}$), 0.87 (3H, t, *J* = 6.0 Hz, H^{15}); ^{13}C NMR (300 MHz, CDCl_3): 64.7, 63.6, 51.0, 47.9, 32.0, 31.1, 29.7, 29.62, 29.57, 29.5, 29.3, 26.5, 22.8, 19.6, 14.3; HRMS (ES): *m/z* = 358.2409; $\text{C}_{17}\text{H}_{37}\text{NO}_3\text{SNa}$ [$\text{M}+\text{Na}$] $^+$ requires 358.2386. ^1H and ^{13}C NMR data in agreement with those previously reported.³

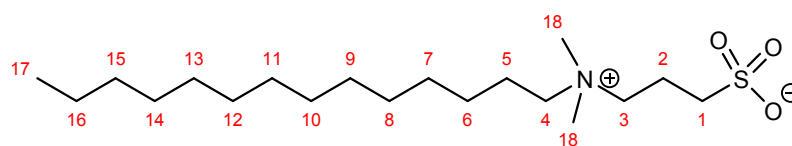
N,N-dimethyltetradecan-1-amine



Under an atmosphere of nitrogen, an ethanolic solution of dimethylamine (5.60 M, 48.0 mL, 270 mmol, 10.0 eq) was added dropwise to a solution of 1-bromotetradecane (8.0 mL, 27 mmol, 1.0 eq) in ethanol (30 mL). The reaction mixture was then heated to 75 °C for 21 hours. After cooling, the reaction solvent was removed under pressure to give a creamy white solid. NaOH (1 M, 60 mL) and hexane (60 mL) were then added, and the aqueous layer further extracted with hexane (3 x 60mL). The combined organic extracts were dried over MgSO₄, filtered, and concentrated down under reduced pressure. This afforded *N,N*-dimethyl-tetradecyl-1-amine as a peach-coloured opaque liquid (5.54 g, 85%).

¹H NMR (300 MHz, CDCl₃): δ_H = 2.27-2.13 (8H, m, H¹, H¹⁵), 1.53-1.35 (2H, m, H²), 1.34-1.15 (22H, m, H³ – H¹³), 0.85 (3H, t, J = 6.6 Hz, H¹⁴); ¹³C NMR (300 MHz, CDCl₃): δ_C = 60.1, 45.6, 32.1, 29.82, 29.77, 29.5, 28.0, 27.6, 22.8, 14.2; HRMS (ES): *m/z* = 242.2880; C₁₆H₃₆N (M+H)⁺ requires 242.2842.¹H NMR data in agreement with those previously reported.²

3-(dimethyl(tetradecyl)ammonio)propane-1-sulfonate



N,N-dimethyl-tetradecyl-1-amine (2.5 mL, 8.3 mmol, 1.0 eq) in acetone (15 mL) was added to a solution of 1,3-propanesulfone (3.6 mL, 41 mmol, 5.0 eq) in acetone (20 mL) refluxed for 5 hours. This afforded a white solid which was filtered at room temperature, washed with acetone and purified *via* recrystallisation with methanol and acetone. This afforded 3-(dimethyl(tetradecyl)ammonio)propane-1-sulfonate as an off-white solid (2.73 g, 92%).

¹H NMR (300 MHz, CDCl₃): δ_H = 3.84-3.70 (2H, m, H³), 3.33-3.09 (8H, m, H⁴, H¹⁸), 2.92 (2H, t, J = 6.7 Hz, H¹), 2.34-2.19 (2H, m, H²), 1.81-1.63 (2H, m, H⁵), 1.39-1.17 (22H, m, H⁶ – H¹⁶), 0.86 (3H, t, J = 6.0 Hz, H¹⁷); ¹³C NMR (300 MHz, CDCl₃): 64.7, 63.6, 50.9, 47.9, 32.1, 31.1, 29.82, 29.79, 29.7, 29.64, 29.58, 29.5, 29.4, 26.5, 22.8, 19.6, 14.3; HRMS (ES): *m/z* = 386.2711; C₁₉H₄₁NO₃SNa (M+Na)⁺ requires 386.2699.¹H NMR data in agreement with those previously reported.⁴

Surface tension of pure and mixed surfactants

The surface tension of the pure surfactants and different mixtures of C₁₂-PC:SB3-12 in choline chloride:glycerol were measured using the procedure presented in the main text. The results of those measurements are presented in Fig. S1 and Fig. S2 for the pure surfactants and mixtures, respectively.

At low concentrations, the surface tension of the different systems decreases with increasing surfactant concentration. Above a certain concentration the surface tension of the system remains constant upon addition of more surfactant. Such a sharp change in the behaviour of the system is the CMC.

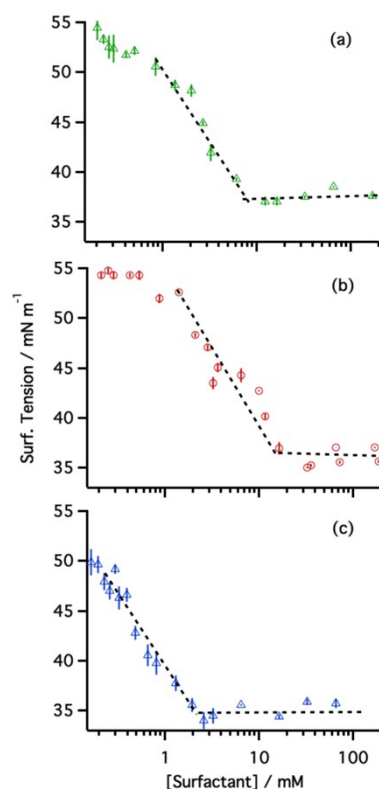


Fig. S1 Surface tension vs. concentration plots of (a) C_{12} -PC, (b) SB3-12 and (c) SB3-14 in choline chloride:glycerol. The error bars are the standard deviation of 5 individual measurements. The black-dashed lines represent the pre- and post-CMC trends used to find the CMC.

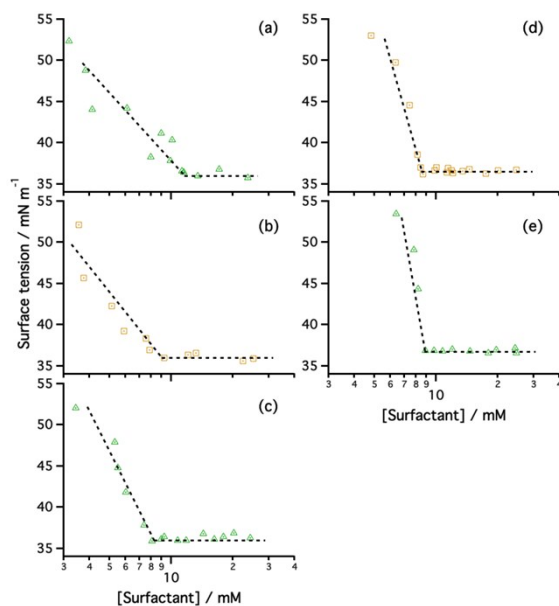


Fig. S2 Surface tension plots of surfactant mixtures at various mole fractions of C_{12} -PC in the surfactant mixture: (a) 0.2, (b) 0.35, (c) 0.5, (d) 0.65 and (e) 0.8. The black-dashed lines represent the pre- and post-CMC trends used to find the CMC.

Molecular volumes, scattering lengths and scattering length densities

The scattering length density (SLD) of each component of the system has been calculated using the scattering length (b) of each unit and the volume that it occupies (V_m). The scattering lengths have been calculated as the atomic contribution to the scattering and the frequency of each atom in the unit: 1:2 choline chloride:glycerol (ChCl:glyc), dodecyl tail ($C_{12}H_{25}$), tetradecyl tail ($C_{14}H_{29}$), sulfobetaine headgroup ($C_5H_{12}NO_3S$) and phosphocholine headgroup ($C_5H_{13}NO_4P$). The values used in our fitting are presented in Table S1.

Table S1 Molecular volumes, scattering lengths and scattering length densities for X-ray and neutrons of each unit within the system.

Unit	$V_m / \text{\AA}^3$	X-ray b / fm	Neutron b / fm	X-ray SLD / $\times 10^{-6} \text{\AA}^{-2}$	Neutron SLD / $\times 10^{-6} \text{\AA}^{-2}$
1:2 h-ChCl:h-glyc	453 ⁵	496	20.5	10.9	0.45
1:2 h-ChCl:d-glyc	453 ⁵	-	187	-	4.1
1:2 h/d-ChCl:h/d-glyc	453 ⁵	-	169	-	3.7
1:2 d-ChCl:d-glyc	453 ⁵	-	281	-	6.2
$C_{12}H_{25}$	350 ^a	273	-13.7	7.8	-0.39
$C_{14}H_{29}$	404 ^a	318	-15.4	7.9	-0.38
$C_5H_{12}NO_3S$	181 ⁶	251	18.0	13.9	0.93
$C_5H_{13}NO_4P$	174 ⁷	273	22.3	15.8	1.3

^aThe molecular volumes of the surfactant tails were calculated using the Tanford equation.⁸

The molecular volumes used for the surfactant tails have been derived from the Tanford equation.⁸ These values have been chosen for the sake of consistency with our previous investigations of surfactant self-assembly in DES,^{5, 9, 10} but they are not the only possible values. In fact these values were derived from measurements “near room temperature” so their validity at different temperatures is limited. There are now many studies in the literature that quote various values for the molecular volumes of aliphatic chains and surfactant headgroups, and some of these include a quantification of the effect of temperature. However, the differences in the molecular volume generally deviate by up to 6 % from Tanford’s value and we consider this to be a minor effect on our fitting, especially since we cannot be sure about the magnitude of the influence that the DES solvent itself has on these values. To show this we have repeated our fitting using some alternative literature values for the molecular volume. Fits for C_{12} -PC using values derived from Tanford ($V_{C_{12}}=350 \text{\AA}^3$),⁸ Nagle *et al.* ($V_{C_{12}}=370.3 \text{\AA}^3$),¹¹ and Armen *et al.* ($V_{C_{12}}=361.6 \text{\AA}^3$),⁷ are compared in Fig. S3.

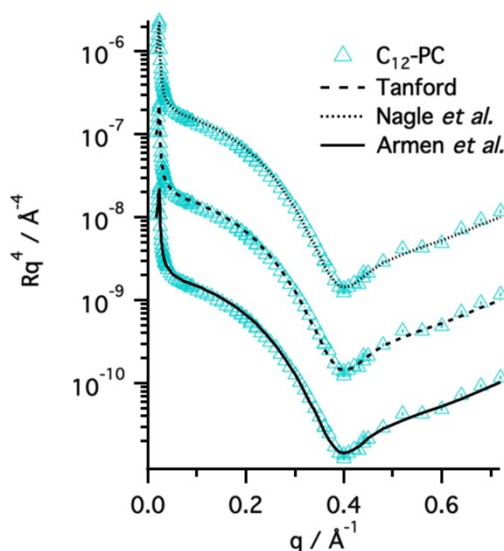


Fig. S3 C_{12} -PC data at the CMC on choline chloride:glycerol and comparison of fits obtained from different SLDs derived from the following molecular volumes of the surfactant tail: 350\AA^3 ,⁸ 370.3\AA^3 ,¹¹ and 361.6\AA^3 .⁷

The main differences in the fits, as expected, appear in the volume fraction of tails in the tail layer, whereas the structural characteristics of the monolayer remain practically unchanged. As the volume of individual tails increase, the SLD decreases, and therefore the volume fraction of tails increases, as they occupy more space without violating any of the physical constraints mentioned in the main text. As those differences are around 2 % at most (See Table S2), we can conclude that the fits using Tanford’s values are as valid in this case as any other choice of volume. Nonetheless, there is undoubtedly some uncertainty in the molecular volume so we have used the variation shown here to define the error in the

values quoted in the main article. A similar consideration is in principle applicable to the head-group volumes with different possible literature values. But to our knowledge, there is no published molecular volume for the phosphocholine head-group in these surfactants. We have therefore used the values from Armen *et al.* obtained from an MD simulation of a lipid bilayer in water, as these allow the calculation of the individual parts of the head-group. i.e. the volume of choline and phosphate can be included but the carboxylic and glycerol groups present in common lipids ignored.⁷ The volume for the sulfobetaine head-group derives from the accurate determination of component volumes of a sulfobetaine micelle in water using contrast-variation SANS.⁶

Table S2 Comparison of tail volume fraction parameter (ϕ_t) when fitted with different tail molecular volumes (V_{C12}).

$V_{C12} / \text{\AA}^3$	$\phi_t / 10^{-2}$
350.0 ⁸	72.0
370.3 ¹¹	75.8
361.6 ⁷	74.1

Solvent contribution to the scattering

As stated in the main text, the solvent contribution to the SANS data was subtracted after data reduction. The scattering from the pure solvents is shown in Fig. S4 for reference.

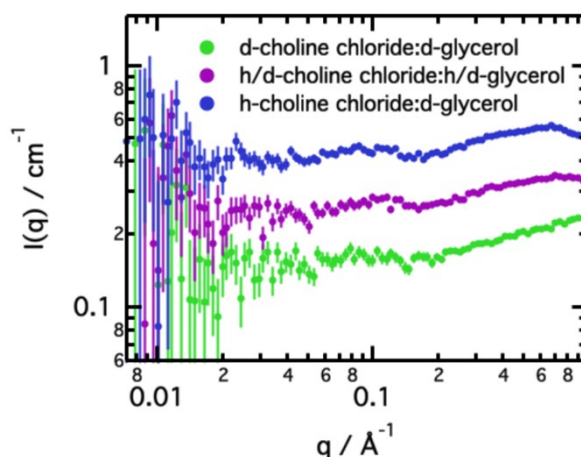


Fig. S4 Scattering contribution of the different isotopic mixtures of pure 1:2 choline chloride:glycerol.

Modelling small-angle neutron scattering data

As introduced in the main text, we have decided to use a homogeneous ellipsoid model to fit the SANS data. This was decided based on the assumption that micelles are in a thermodynamic equilibrium, as previously proposed for other micelles in DES,^{5, 10} and on the goodness of fit using such a model. In order to find the most likely conformation of micelles in solution we have compared the quality of the fits through the statistic (χ^2 / N_{pts} , where N_{pts} is the number of data points), which decreases when the quality of the fit improves. Three different mathematical models have been compared here: monodisperse spheres, polydisperse spheres and monodisperse ellipsoids. Fig. S5 presents the SANS data for C_{12} -PC micelles in choline chloride:glycerol DES at different surfactant concentrations, together with the fits using different models. Table S3 shows the Chi square values for each of the models.

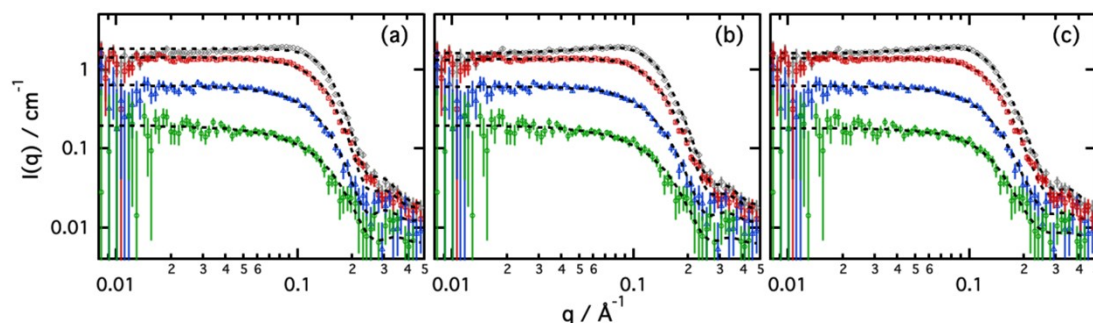


Fig. S5 SANS data and best fits of C_{12} -PC micelles in choline chloride:glycerol at different surfactant concentrations. Those concentrations are quoted in the main text and in Table S3. The fits, represented by black-dashed lines,

correspond to the following models: (a) monodisperse spheres, (b) polydisperse spheres and (c) monodisperse ellipsoids.

Table S3 χ^2 / N_{pts} statistic for the different models used to fit the data presented in Fig. S2.

C_{12} -PC concentration / mM	Monodisperse spheres	Polydisperse spheres	Monodisperse ellipsoids
31.5±1.2	0.63	0.61	0.50
68.1±2.4	0.90	0.8	0.77
134±3	2.7	1.4	0.82
308±2	9.8	2.3	0.93

Although improvements can be hardly observed by visual inspection, Chi Square statistics indicate differences between the models. In that sense, the monodisperse ellipsoids model was found to be the best model to fit these data, particularly at high surfactant concentrations.

X-ray reflectivity results of surfactant mixtures

The characteristics of the adsorbed layer of mixed surfactants were determined by means of X-ray reflectivity. The results from those fits are presented in Table S4 and the plots from those fits can be found in the main text. The interfacial roughnesses associated to the models were fitted to values between 3.5 Å and 5.0 Å.

Table S4 X-ray reflectivity results of zwitterionic mixtures at the CMC. A 2-layer and subphase model was used to fit the data as presented in Fig. 7. The error bars were obtained from the Motofit fits by individually varying each parameter to produce a substantial increase in the Chi Square parameter of the fit. Such variation was used as the error associated to the parameter.

C_{12} -PC/SB3-12	t_t / Å	ϕ_t	t_h / Å	ϕ_h	$\Gamma_{S,CMC} / \times 10^{-6} \text{ mol m}^{-2}$	APM / Å ²
0.2/0.8	7.8±0.3	0.73±0.04	5.7±0.3	0.50±0.04	2.6±0.2	63±4
0.35/0.65	7.8±0.3	0.78±0.03	5.8±0.2	0.52±0.02	2.8±0.1	59±3
0.5/0.5	8.0±0.2	0.79±0.03	5.9±0.2	0.53±0.03	2.8±0.1	57±3
0.65/0.35	8.6±0.3	0.77±0.03	6.3±0.2	0.52±0.03	2.9±0.1	54±3
0.8/0.2	8.5±0.2	0.77±0.04	6.5±0.2	0.49±0.02	2.9±0.2	55±4

Small-angle neutron scattering results

Uniform ellipsoid modelling

The plots for all the SANS contrasts used to determine the structure of pure surfactant micelles in choline chloride:glycerol are presented below: C_{12} -PC – Fig. S6, SB3-12 – Fig. S7 and SB3-14 – Fig. S8. The results from the simultaneous fit of those contrasts are presented in Table S5, S6 and S7.

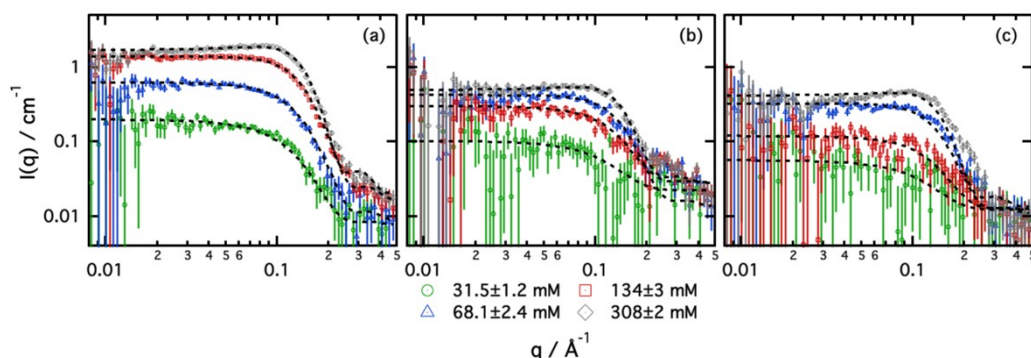


Fig. S6 SANS data and best fits of h- C_{12} -PC in (a) d-choline chloride:d-glycerol, (b) h/d-choline chloride:h/d-glycerol and h-choline chloride:d-glycerol at different surfactant concentration (as shown in the legend).

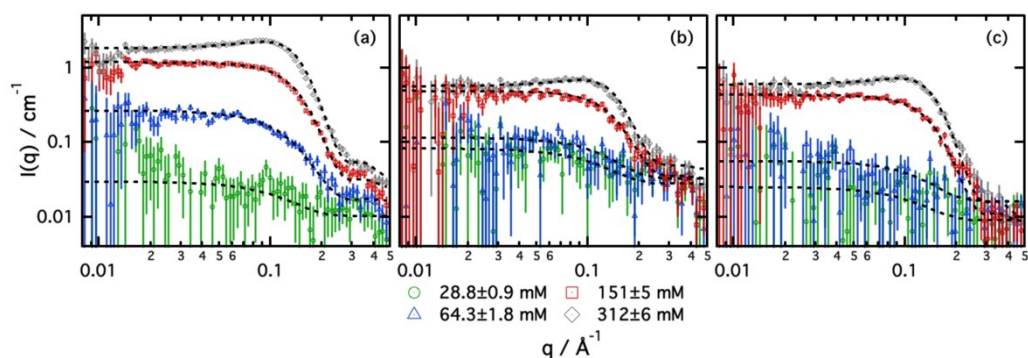


Fig. S7 SANS data and best fits of h-SB3-12 in (a) d-choline chloride:d-glycerol, (b) h/d-choline chloride:h/d-glycerol and h-choline chloride:d-glycerol at different surfactant concentration (as shown in the legend).

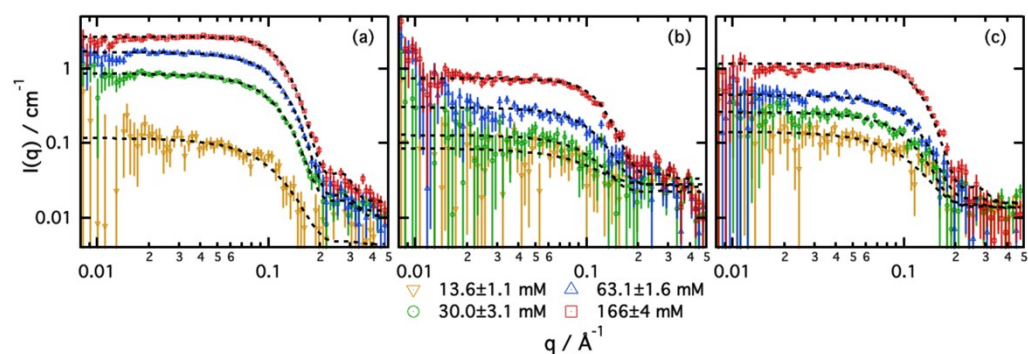


Fig. S8 SANS data and best fits of h-SB3-14 in (a) d-choline chloride:d-glycerol, (b) h/d-choline chloride:h/d-glycerol and h-choline chloride:d-glycerol at different surfactant concentration (as shown in the legend).

Table S5 Fitting parameters derived from the SANS data at different concentrations of C₁₂-PC in choline chloride:glycerol.

Conc / mM	r_{eq} / Å	AR	R_g / Å	$\phi_{fit} / 10^{-2}$	$\phi_{S(q)} / 10^{-2}$	R_{eff} / Å
31.5±1.2	16±2	2.3±0.3	19±2	0.27±0.02	1.6±1.4	21±1
68.1±2.4	16±1	1.9±0.2	17±1	0.90±0.05	7.3±1.8	20±1
134±3	16±1	1.9±0.1	17±1	2.6±0.4	12±2	19±1
308±2	15±1	1.9±0.1	17±1	4.4±0.2	15±1	19±1

Table S6 Fitting parameters derived from the SANS data at different concentrations of SB3-12 in choline chloride:glycerol.

Conc / mM	r_{eq} / Å	AR	R_g / Å	$\phi_{fit} / 10^{-2}$	$\phi_{S(q)} / 10^{-2}$	R_{eff} / Å
28.8±0.9	14±2	1.7±0.6	15±2	0.03±0.02	0.9±0.8	18±1
64.3±1.8	14±1	1.8±0.2	15±1	0.40±0.02	2.8±1.1	18±1
151±5	15±1	1.7±0.1	16±1	2.2±0.2	8.3±4.3	19±1
312±6	15±1	1.7±0.1	15±1	5.7±0.1	14±1	18±1

Table S7 Fitting parameters derived from the SANS data at different concentrations of SB3-14 in choline chloride:glycerol.

Conc / mM	r_{eq} / Å	AR	R_g / Å	$\phi_{fit} / 10^{-2}$	$\phi_{S(q)} / 10^{-2}$	R_{eff} / Å
13.6±1.1	18±1	1.9±0.6	19±4	0.09±0.02	3.7±2.5	22±1
30.0±3.1	20±1	1.6±0.1	19±1	0.7±0.2	5.8±5.5	23±1
63.1±1.6	19±1	1.7±0.1	19±1	1.6±0.1	7.1±2.4	23±1
166±4	19±1	1.6±0.1	19±1	3.2±0.1	9.7±1.5	23±1

Core-shell ellipsoid modeling

As indicated in the main text, one of the high surfactant concentrations was fitted using a core-shell ellipsoidal model. The AR was fixed to the value obtained through the modeling using the uniform ellipsoid model. The thickness of the headgroup layer obtained in reflectivity was used as an initial guess of the size of the headgroup region. The R_{eff} was recalculated for the new micelle morphology. Finally, core radius ($r_{eq,core}$), shell thickness ($t_{eq,shell}$), volume fraction of micelles ($\phi_{P(q)}$) and interaction ($\phi_{S(q)}$) were fitted to the data, and volume fraction of the headgroup in the solvated layer (ϕ_{hg}) were obtained through co-refinement of the three contrasts. Fig. S9 contains the SANS data and fits, and Table S8 shows the results from those fits.

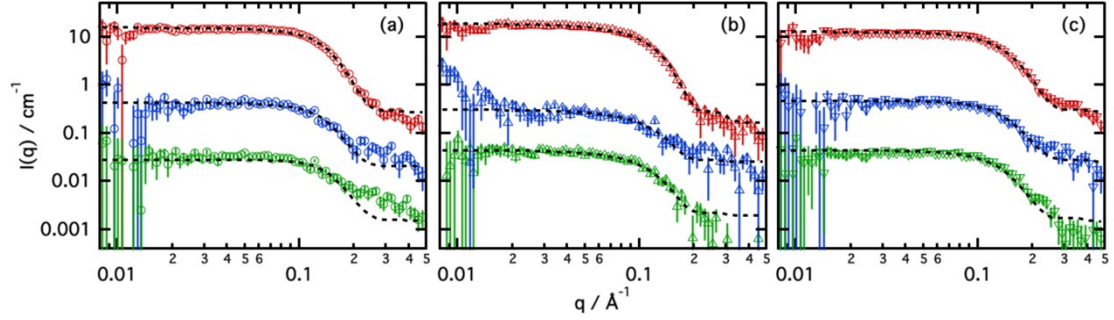


Fig. S9 SANS data (markers) and best fits (black-dashed lines) of (a) C₁₂-PC, (b) SB3-12 and (c) SB3-14 micelles in 1:2 choline chloride:glycerol. Three different contrasts were measured and simultaneously fitted to a core-shell ellipsoid model: (red markers) protonated surfactant in d-choline chloride:d-glycerol, (blue markers) protonated surfactant in h/d-choline chloride:h/d-glycerol, and (green markers) protonated surfactant in h-choline chloride:d-glycerol.

Table S8 Fitting parameters derived from the SANS data presented in Fig. SXX. A core-shell ellipsoid model has been used to obtain these.

Surfactant	Conc. /mM	$r_{eq,core} / \text{\AA}$	AR	$t_{eq,shell} / \text{\AA}$	$\phi_{hg} / 10^{-2}$	$\phi_{P(q)} / 10^{-2}$	$\phi_{S(q)} / 10^{-2}$	$R_{eff} / \text{\AA}$
C ₁₂ -PC	134±3	14±1	2.0±0.1	7±1	29±8	4.3±0.8	13±2	26±1
SB3-12	151±5	14±1	1.7±0.1	5±1	12±11	4.60±0.9	7.1±1.4	23±1
SB3-14	63.1±1.6	19±1	1.7±0.1	5±1	27±6	2.0±0.7	12±2	29±1

Modelling of surfactant mixtures

SANS data of the surfactant mixtures (C_{12} -PC/SB3-12) at two total surfactant concentrations (72.3 ± 1.2 and 185 ± 3) were fitted using one contrast, following the procedure presented in the main text. Fig. S10 shows the SANS data and best fits of different surfactant ratios at a total surfactant concentration of 72.3 ± 1.2 , whereas the second dataset is included in the main text.

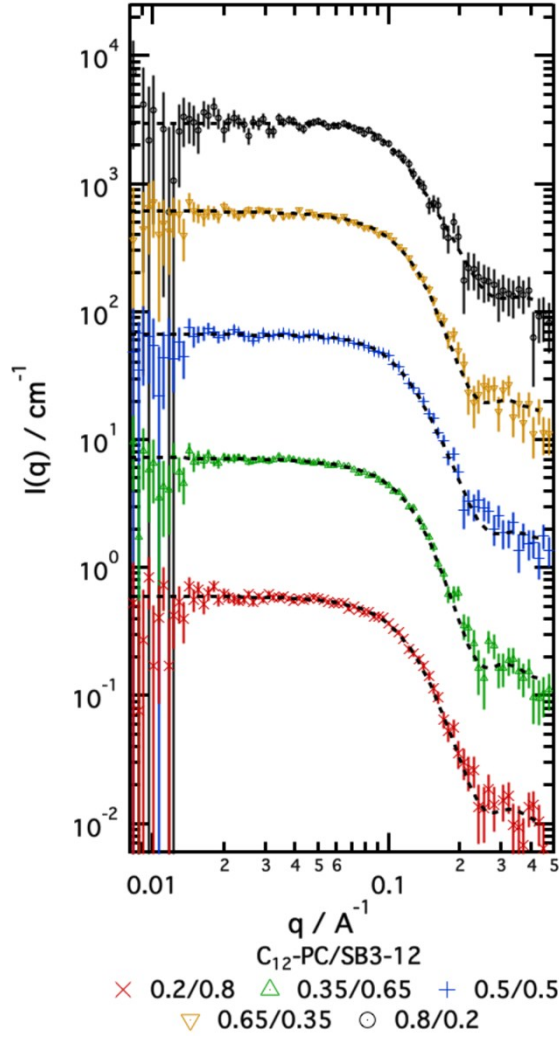


Fig. S10 SANS data and best fits (black-dashed lines) of different mole fractions of surfactant in a C_{12} -PC/SB3-12 mixture at a total surfactant concentration of 72.3 ± 1.2 mM. The mole fractions of C_{12} -PC in the surfactant mixture are presented in the legend of the graph. The intensity of data and fits has been offset for clarity.

The results from those fits are included in Table S8.

Table S9. Results from the individual fits of two concentrations of different surfactant mixtures of C_{12} -PC and SB3-12.

C_{12} -PC/SB3-12	$r_{eq} / \text{\AA}$	AR	$\phi_{fit} / 10^{-2}$	$\phi_{S(q)} / 10^{-2}$	$R_{eff} / \text{\AA}$
72.3 ± 1.2					
0.2/0.8	16 ± 1	1.7 ± 0.2	0.5 ± 0.2	6.7 ± 1.7	19 ± 1
0.35/0.65	16 ± 1	1.8 ± 0.2	0.8 ± 0.1	7.3 ± 1.2	20 ± 1
0.5/0.5	16 ± 1	1.9 ± 0.1	0.9 ± 0.1	6.6 ± 0.9	20 ± 1
0.65/0.35	16 ± 1	2.1 ± 0.4	1.0 ± 0.1	7.6 ± 1.1	21 ± 1
0.8/0.2	16 ± 1	2.0 ± 0.2	0.8 ± 0.1	6.2 ± 1.1	20 ± 1
185 ± 3					
0.2/0.8	16 ± 1	1.7 ± 0.1	3.3 ± 0.1	11 ± 1	19 ± 1
0.35/0.65	16 ± 1	1.8 ± 0.1	3.2 ± 0.1	10 ± 1	19 ± 1
0.5/0.5	16 ± 1	1.8 ± 0.1	3.4 ± 0.1	10 ± 1	20 ± 1
0.65/0.35	16 ± 1	1.9 ± 0.1	3.2 ± 0.1	9.8 ± 0.8	20 ± 1
0.8/0.2	16 ± 1	1.9 ± 0.1	3.5 ± 0.1	9.9 ± 0.9	20 ± 1

References

1. Brycki, B.; Szafran, M. Effect of pH on carbon-13 NMR spectra of N-dodecyl-N, N-dimethylamine oxide solution. *Magn. Reson. Chem.* **1992**, *30* (6), 535-543.
2. Xu, D.; Ni, X.; Zhang, C.; Mao, J.; Song, C. Synthesis and properties of biodegradable cationic gemini surfactants with diester and flexible spacers. *J. Mol. Liq.* **2017**, *240*, 542-548.
3. He, L.; Qin, S.; Chang, T.; Sun, Y.; Gao, X. Biodiesel synthesis from the esterification of free fatty acids and alcohol catalyzed by long-chain Bronsted acid ionic liquid. *Catal. Sci. Technol.* **2013**, *3* (4), 1102-1107.
4. Qu, G.; Cheng, J.; Wei, J.; Yu, T.; Ding, W.; Luan, H. Synthesis, Characterization and Surface Properties of Series Sulfobetaine Surfactants. *J. Surfactants. Deterg.* **2011**, *14* (1), 31-35.
5. Sanchez-Fernandez, A.; Arnold, T.; Jackson, A. J.; Fussell, S. L.; Heenan, R. K.; Campbell, R. A.; Edler, K. J. Micellization of alkyltrimethylammonium bromide surfactants in choline chloride:glycerol deep eutectic solvent. *Phys. Chem. Chem. Phys.* **2016**, *18* (48), 33240-33249.
6. Holdaway, J. A. A study of the structure and formation of biocompatible mesostructured polymer-surfactant hydrogel films. *University of Bath* **2013**, *PhD thesis*.
7. Armen, R. S.; Uitto, O. D.; Feller, S. E. Phospholipid component volumes: determination and application to bilayer structure calculations. *Biophys. J.* **1998**, *75* (2), 734-744.
8. Tanford, C. Micelle shape and size. *J. Phys. Chem.* **1972**, *76* (21), 3020-3024.
9. Sanchez-Fernandez, A.; Edler, K. J.; Arnold, T.; Heenan, R. K.; Porcar, L.; Terrill, N. J.; Terry, A. E.; Jackson, A. J. Micelle structure in a deep eutectic solvent: a small-angle scattering study. *Phys. Chem. Chem. Phys.* **2016**, *18* (20), 14063-73.
10. Sanchez-Fernandez, A.; Hammond, O. S.; Jackson, A. J.; Arnold, T.; Douth, J.; Edler, K. J. Surfactant-solvent interaction effects on the micellization of cationic surfactants in a carboxylic acid-based deep eutectic solvent. *Langmuir* **2017**, *33* (50), 14304-14314.
11. Petrache, H. I.; Feller, S. E.; Nagle, J. F. Determination of component volumes of lipid bilayers from simulations. *Biophys. J.* **1997**, *72* (5), 2237-2242.